Published in final edited form as:
J Neurochem. 2012 November ; 123(2): 276–287. doi:10.1111/j.1471-4159.2012.07912.x.

Comparative peptidomics analysis of neural adaptations in rats repeatedly exposed to amphetamine

Elena V. Romanova[1], **Ji Eun Lee**[1,5], **Neil L. Kelleher**[2], **Jonathan V. Sweedler**[1,3,*], and **Joshua M. Gulley**[3,4,*]

[1]Department of Chemistry and the Beckman Institute, University of Illinois at Urbana-Champaign, 600 S. Mathews Ave., Urbana, IL 61801, USA

[2]Department of Chemistry, Department of Molecular Biosciences, and The Chemistry of Life Processes Institute, Northwestern University, 2145 Sheridan Rd., Evanston, IL USA

[3]Neuroscience Program, University of Illinois at Urbana-Champaign, 505 South Goodwin Avenue, Urbana, IL 61801, USA

[4]Department of Psychology, University of Illinois at Urbana-Champaign, 603 E. Daniel St., Champaign, IL 61820, USA

Abstract

Repeated exposure to amphetamine (AMPH) induces long-lasting behavioral changes, referred to as sensitization, that are accompanied by various neuroadaptations in the brain. To investigate the chemical changes that occur during behavioral sensitization, we applied a comparative proteomics approach to screen for neuropeptide changes in a rodent model of AMPH-induced sensitization. By measuring peptide profiles with matrix-assisted laser desorption/ionization time-of-flight mass spectrometry and comparing signal intensities using principal component analysis and variance statistics, subsets of peptides are found with significant differences in the dorsal striatum, nucleus accumbens and medial prefrontal cortex of AMPH-sensitized male Sprague-Dawley rats. These biomarker peptides, identified in follow-up analyses using liquid chromatography and tandem mass spectrometry, suggest that behavioral sensitization to AMPH is associated with complex chemical adaptations that regulate energy/metabolism, neurotransmission, apoptosis, neuroprotection, and neuritogenesis, as well as cytoskeleton integrity and neuronal morphology. Our data contribute to a growing number of reports showing that in addition to the mesolimbic dopamine system, which is the best known signaling pathway involved with reinforcing the effect of psychostimulants, concomitant chemical changes in other pathways and in neuronal organization may play a part in the overall effect of chronic AMPH exposure on behavior.

Keywords

Mass spectrometry; proteomics; principal component analysis; addiction; peptidomics; neurochemical adaptation

*To Whom Correspondence should be addressed: Jonathan V. Sweedler, jsweedle@illinois.edu. Joshua M. Gulley, jgulley@illinois.edu.
[5]Current address: Center for Theragnosis, Korea Institute of Science and Technology, Seoul, Korea

Author contributions. Romanova played the major role in experimental design, MALDI and LC-MS experiments, data interpretation and manuscript preparation; Lee performed the FTMS studies and associated data analysis; Kelleher aided the FTMS studies, data interpretation and manuscript editing; Sweedler aided experimental design, data interpretation, and manuscript preparation, and with Gulley, initiated the study; in addition, Gulley helped with the experimental design, performed the behavioral studies and interpreted the behavioral data, and contributed to manuscript revision. All authors approved the final version of the manuscript and have no conflict of interest to declare.

Introduction

The repeated use of stimulant drugs such as amphetamine (AMPH) leads to long-lasting changes in behavior. For example, sensitization, which is an enhanced responsiveness to a drug on subsequent exposures, has been described in humans for AMPH- and methamphetamine-induced psychosis (Robinson & Berridge 1993, Bartlett *et al.* 1997, Ujike & Sato 2004) and AMPH-induced euphoria, drug "liking" and motor activation (Strakowski *et al.* 2001, Boileau *et al.* 2006). Moreover, sensitization has been hypothesized to contribute to the development of compulsive behaviors that characterize addiction (Kalivas *et al.* 1998, Robinson & Berridge 1993). Drug-induced sensitization has been successfully modeled in animals; specifically, in rats and mice, repeated but intermittent exposure to AMPH typically leads to progressive and long-lasting augmentation of species-specific motor behaviors such as locomotion, head movement and sniffing, and stereotyped (i.e., repetitive) head, limb, and orofacial movements (Segal & Schuckit 1983). An extensive literature search suggests that the mesencephalic dopamine system, which includes cell bodies in the substantia nigra and ventral tegmental area (VTA) that terminate largely in the dorsal striatum (dSTR), nucleus accumbens (NAc) and prefrontal cortex (PFC), is a critical component of the neural circuitry that underlies both behavioral sensitization and addiction (Robinson & Berridge 2000). Accordingly, this has led us to investigate the neuroadaptations resulting from repeated drug exposure in specific brain regions that govern the behavioral sensitization processes.

Mass spectrometry (MS)-based approaches are proving efficacious for the analysis and identification of signaling proteins and protein signatures associated with repeated exposure to drugs of abuse in animal models and human addicts (Romanova *et al.* 2009, Zvonok *et al.* 2010, Uys *et al.* 2010, Abul-Husn & Devi 2006, Rossbach *et al.* 2009, Faure *et al.* 2009, Yang *et al.* 2008b). Likewise, clinical MS is pushing comparative metabolomic and proteomic matrix-assisted laser desorption/ionization (MALDI) profiling for diagnostic purposes (Rajalahti *et al.* 2010, Hanrieder *et al.* 2011, Darde *et al.* 2010). Using comparative mass spectrometric profiling aided by biostatistics and mass spectrometric sequencing, we ascertained that a broad range of endogenous peptides change their levels in reward-related brain regions of rats with AMPH-induced behavioral sensitization. Specifically, we employed two MS ionization approaches: direct MALDI for relative quantitation of peptides from large numbers of small-volume samples, and electrospray ionization (ESI) combined with high performance liquid chromatography (HPLC) to identify and characterize the observed MS peaks (Fenn *et al.* 1989, Hillenkamp & Karas 2007). MALDI-time-of-flight (TOF) MS is used for robust, label-free analysis of raw tissue extracts, primarily due to its high tolerance to salts. Importantly, the small-volume sample requirements inherent to MALDI-TOF MS make it well suited for measuring peptides from individual small brain regions, thereby offering the potential capability to correlate individual behavioral data with region-specific peptide profiles. We used a one-step sample preparation approach for the extraction of peptides from brain tissue using prolonged tissue incubations in 2,5-dihydroxybenzoic acid (DHB) (Romanova *et al.* 2008), a method that has been successfully combined with MALDI-TOF MS to identify peptides associated with a heightened sensitivity to cocaine (Romanova *et al.* 2010). By implementing this approach we profiled peptide extracts from brain regions of individual rats and compared profiles using principal component analysis (PCA) (Brereton 2009), which reduced the dimensionality of the MS data and revealed unique AMPH-induced trends in the peak patterns in dSTR, NA and mPFC tissues.

Because MALDI-TOF MS consumes a small fraction of the sample, the altered peaks were characterized with a more conventional peptidomics approach, multi-stage HPLC coupled to

ESI-tandem MS (MS/MS) (Svensson *et al.* 2007, Fricker *et al.* 2006, Li & Sweedler 2008, Wei *et al.* 2006), from a pooled sample created by combining the unused portions of the individual extracts (Fig 1). In this way, different subsets of endogenous peptides originating from known proteins have been identified in individual animals. Our data suggest that there are alterations in energy metabolism, neuroprotection pathways, neuronal structure and cytoskeleton integrity that correlate with AMPH-induced behavioral sensitization in rats.

Experimental procedures

Animals

Male Sprague-Dawley rats (n = 12), which were the offspring of breeder rats purchased from Harlan Laboratories (Indianapolis, IN, USA) and maintained in our animal facility, were housed individually starting at ~2 months of age in an acrylic tub (46 × 25 × 22 cm) lined with hardwood bedding. Rats, which were 2.5–3 months old at the start of experiments, were maintained on a 12:12 h light:dark cycle (lights on at 08:00) with food and water available *ad libitum*. Prior to being used in the study, rats were handled on five separate occasions for 15 min. Animal care, euthanasia and all other experimental procedures were approved by the Institutional Animal Care and Use Committee, University of Illinois at Urbana-Champaign, and were consistent with the *Principles of Laboratory Animal Care* (NIH Publication no. 85-23); in addition, the ARRIVE guidelines have been followed.

Repeated saline or AMPH treatment and behavioral measures

Tests of saline- and AMPH-induced changes in locomotor activity were performed in four separate open-field activity chambers as described previously (Stanis *et al.* 2008). Rats were first habituated to the procedure by placing them in the open-field arena for 30 min. They were then removed, injected with saline (1 ml/kg, intraperitoneal (i.p.)), and returned to the arena for 60 min. On the next day (i.e., treatment day 1), the same procedure was repeated, except one group of rats (n = 4) was randomly chosen to receive an injection of saline and the remainder (n = 8) were given an i.p. injection of *d*-AMPH sulfate (3.0 mg/kg; dose calculated based on the weight of the salt). Beginning on treatment day 2 and continuing on alternating days until treatment day 9, rats were brought to the laboratory, injected with saline or AMPH, and allowed to behave for 60 min in an acrylic tub (46 × 25 × 22 cm) lined with hardwood bedding. On treatment day 10, the open-field testing procedure used on treatment day 1 was repeated. Thus, rats received a total of 10 saline or AMPH injections (cumulative dose = 30 mg/kg) over the course of 19 d, with automated (i.e., photobeam) activity measures obtained on the first and final injection days. Two dependent measures of behavior were taken from the activity monitoring software (TruScan, v 2.0; Coulbourn Instruments, Whitehall, PA, USA). The first was ambulation, which was calculated by tabulating consecutive photobeam breaks and converting this to distance (in meters). The second was stereotypy, which is a measure of repetitive behavior such as head and body swaying, head bobbing, and sniffing, and is calculated by tabulating repetitive beam breaks in a focused area that do not contribute to large changes in location in the open-field. The statistical significance of group differences in activity following injection was determined using three-way, mixed factor ANOVA (group × injection number × time post-injection) followed by post-hoc analysis with two-way ANOVA and Tukey tests. To analyze the relationship between individual differences in AMPH-induced sensitization and MS peptide profiles, a sensitization index was also calculated for each AMPH-exposed rat. This was obtained by dividing the cumulative ambulation or stereotypy value for the 60 min following the tenth injection by the same value following the first injection. Thus, values above 1 are indicative of sensitization. The statistical significance of group differences in these measures

was determined using one-way ANOVA. Mean behavioral scores were then analyzed against MS peptide profiles using PCA.

Tissue sampling and peptide extraction

Immediately following their removal from the open-field arena, rats were euthanized by rapid decapitation. Their brains were carefully removed, rinsed in ice-cold 0.9% saline, sliced in 2 mm coronal sections with the assistance of a calibrated brain matrix, and placed on a glass dish kept on ice. Within 1.5–3 min after decapitation, samples of the ventral mPFC and the core and shell regions of the NAc and dSTR, were isolated from these slices via biopsy punches of different diameters (0.75 mm – mPFC; 1.2 mm–NAc; 2.0 mm – dSTR). Punches were centered on brain regions at the approximate stereotaxic coordinates (Paxinos & Watson 2007) of 3.80 AP, 0.5 ML, and 3.8 DV for mPFC; 1.5 AP, 0.8 ML, 7.6 DV for NAc; and 1.5 AP, 2.6 ML, 5.0 DV for dSTR. The resulting individual tissue samples had a standard volume of 0.86 mm^3, 2.2 mm^3, and 6.2 mm^3 respectively. A total of 72 tissue samples (12 rats × 3 brain regions × 2 hemispheres) were collected from the two groups of rats. For peptide extraction, bilateral tissue punches from each animal were combined and placed in 15, 20 or 30 μL volumes of DHB (20 mg/mL) optimized in initial experiments for the mPFC, NAc and dSTR regions respectively, and incubated for 48 h to maximize peptide extraction as described elsewhere (Romanova et al. 2008). Thus, a total of 36 extracts were used for the peptide profiling experiments described below.

Analysis of peptide profiles by MALDI-TOF MS

For peptide measurements, peptide extracts were spotted on a stainless steel MALDI target in technical duplicates, 0.7 μl per spot, and co-crystallized with 0.7 μL of freshly prepared concentrated DHB matrix (50 mg/mL, in a 50% water/acetone mix). Positive ion mass spectra for all samples were acquired manually in the *m/z* 800–6000 region using a Bruker Ultraflex II mass spectrometer (Bruker Daltonics, Billerica, MA, USA) in reflectron mode with external calibration. Given the microliter volumes of the extraction solutions and the small volumes consumed in each of the MALDI measurements, we performed technical replicates for each sample, leaving sufficient material for the peptide characterizations via a pooled sample, as described below.

Statistical data analysis

The raw MALDI MS data were imported into ClinProTools 2.2 software (Bruker Daltonics), with an *m/z* 1000–5000 mass filter, corrected with the Convex Hull method for a baseline flatness of 0.1, processed by five cycles of the Savitzky–Golay method over an *m/z* 1.0 width to smooth isotopic envelopes, normalized to total ion count, and scaled. For peak picking, spectra from technical duplicates were combined into a representative sample spectrum. Average centroid peaks were selected based on maximal intensity in the mean spectrum of the entire group with a signal-to-noise cut-off of 5 in order to improve meaningful peak peaking. The PCA reduced the dimensionality of the data, with the resultant principal components (PCs) each representing a set of linearly uncorrelated *m/z* values. To create the PCs, the following peak restrictions were applied: the 50 most-intense peaks for dSTR and NA, and 100 most-intense peaks for mPFC. Following PCA, peptide profiles of the mean spectra were compared by the Anderson-Darling normality test and ANOVA or *t*-test (depending on the number of groups compared) for normal distributed data (Stephens 1974). Data not showing normal distribution ($p_{AD} \leq 0.05$) were evaluated by the Wilcoxon/Kruskal-Wallis tests, respectively (Wilcoxon 1945, Kruskal & Wallis 1952). To decrease the number of false positives, the Benjamini-Hochberg method as incorporated into ClinProTools, was automatically applied for p-value adjustment during analysis (Dudoit & Shaffer 2003).

Peptide identification by LC-MS/MS

Following MALDI MS profiling of the individual samples, the remaining peptide extracts from the individual samples were pooled together (e.g., all brain regions from all animals), and this combined sample (of about 730 μL) was processed for peptide identification as described previously (Romanova et al. 2010). Briefly, a significant portion of the DHB was removed from the extracts by solid phase extraction (SPE) prior to multi-stage reversed phase (RP)-liquid chromatography (LC) separation of peptides. Initial fractionation of the SPE-purified extract was done on a Magic 2002 system (Michrom Bioresources, Sacramento, CA, USA) using a C18 microbore column and gradient of solvent A: 95% H_2O, 5% acetonitrile (ACN), 0.1 formic acid (FA), 0.01% heptafluorobutyric acid (HFBA); and solvent B: 95% ACN, 5% H_2O, 0.1% FA, 0.01% HFBA. Complex LC fractions were scanned by MALDI-TOF MS and fractions containing peptides matching by mass to those with higher loading scores from our PCA measures were subjected to a 2^{nd} stage separation with on-line mass spectrometric sequencing. Two different LC-MS/MS platforms were used for sequencing the second stage fractions to improve the number of peaks characterized.

Capillary liquid chromatography (capLC)-ESI-ion trap (IT)-MS/MS

The first system used to characterize the fractions was the HCT Ultra-PTM Discovery system IT mass spectrometer (Bruker Daltonics) equipped with an ESI source. In the capLC-ESI-IT-MS/MS experiments, peptide fractions were eluted from a capillary column (LC Packings, Sunnyvale, CA, USA), 300-μm inner diameter × 15 cm, C18 PepMap100, 100 Å, using optimized solvent gradients at a 2.5 μL/min flow rate (solvent A: 95% H_2O, 5% MeOH, 0.1% FA; solvent B: 95% MeOH, 5% H_2O, 0.1% FA). The MS data was acquired in a data-dependent manner with the dynamic precursor ion exclusion set to 3 spectra for each of the 3 parent ions selected by intensity during 60 s. The fragmentation spectra were analyzed against the NCBI and MSDS protein databases using Biotools 3.0 (Bruker Daltonics) and the Mascot server (Matrix Science, Boston, MA, USA) within the *Rattus* taxonomy. Only peptides identified with ion scores that fell within the significance threshold of 0.05 are reported. The following search parameters were used: (i) enzyme – none; (ii) fixed modification – none, (iii) variable modifications – oxidation (M), acetylation-N – amidation-C; (iv) peptide mass tolerance – 0.5 Da; (v) tandem mass spectrometry mass tolerance – 0.5 Da; (vi) peptide charge – +1, +2, +3; (vii) instrument – ion trap; (viii) allowing up to two missed cleavages. For identifying peptides related to known prohormones, database searching was repeated on fragmentation peak lists exported in the form of a Mascot generic file format against an NCBI database of the rat peptide prohormones using Peaks Studio 4.6 (Bioinformatics Solutions, Waterloo, ON, Canada). The search parameters for the Peaks software included: (i) unsuspected cleavage site, (ii) N-terminal pyro-glutamic acid, disulfide bonds, acetylation and C-terminal amidation, (iii) and mass tolerances of 0.5 Da and 0.3 Da for precursor and fragment ions, respectively. Results generated by Peaks Studio were verified by manual *de novo* analysis using Data Analysis 4.0 and Biotools 3.0 (Bruker Daltonics).

NanoLC-nanoESI-Fourier transform (FT) MS/MS

The second system used was a 12 Tesla LTQ-FT Ultra mass spectrometer (ThermoFisher Scientific, Waltham, MA, USA), interfaced to a 1D NanoLC pump (Eksigent Technologies, Dublin, CA, USA). The sample was analyzed on a ProteoPep™ II column (C_{18}, 300 Å, 5 μm, New Objective, Woburn, MA, USA). The operating flow rate was 300 nl/min (solvent A: 95% H_2O, 5% ACN, 0.2% FA; solvent B: 95% ACN, 5% H_2O, 0.2% FA). Data acquisition on the LTQ-FT instrument consisted of a full scan event (90,000 resolving power), and data-dependent collision-induced dissociation MS/MS scans (40,000 resolving power) of the five most abundant peaks from the previous full scan. The resulting LC-FTMS/MS files (*.raw) were analyzed using neuroProSight (http://

neuroprosight.scs.illinois.edu/) and ProSightPC 2.0 (Thermo Fisher Scientific) (Boyne *et al.* 2009). The ProSight experimental data, each consisting of the monoisotopic neutral masses of precursor species and a list of monoisotopic neutral fragment masses, were searched in a "neuropeptide" search mode (no protease specificity) against an intact rat database (UniProt 15.0, 4318021 protein forms) with a 100 Da precursor and 10 ppm fragment mass tolerance (Lee *et al.* 2010). The Sequence Gazer tool in ProSight was used for manually determining post-translational modifications on the identified peptides.

Results

AMPH-induced behavioral sensitization

Consistent with previous reports (Robinson *et al.* 1985, Stanis et al. 2008), we found that repeated exposure to AMPH lead to significant changes in AMPH-induced ambulation and stereotypy after the tenth injection as compared to the first (Fig. 2). For ambulation, three-way ANOVA revealed significant main effects of group ($F_{1,10} = 35.8$, $p < 0.001$) and time post-injection ($F_{11,110} = 4.21$, $p < 0.001$), along with a time post-injection × injection number interaction ($F_{11,110} = 2.47$, $p < 0.01$). As shown in Fig. 2A, ambulation was significantly greater in AMPH-injected compared to saline-injected rats following the first and tenth treatments. Moreover, ambulatory behavior following the tenth AMPH injection had a biphasic pattern characterized by a more rapid and sharp increase in activity that was followed within 20 min by a reduction in ambulation relative to the first AMPH exposure. This reduction was attributable to a sharp increase in stereotypy. For stereotypy, three-way ANOVA revealed significant main effects of group ($F_{1,10} = 75.5$, $p < 0.001$), time post-injection ($F_{11,110} = 4.60$, $p < 0.001$), and injection number ($F_{1,10} = 8.22$ $p < 0.05$). There were also significant group × time post-injection ($F_{11,110} = 9.03$, $p < 0.001$), group × injection number ($F_{1,10} = 7.90$, $p < 0.05$), and group × time post-injection × injection number ($F_{11,110} = 2.66$, $p < 0.01$) interactions. As shown in Fig. 2B, stereotypy was significantly elevated for the last 45 min of the testing sessions following both the first and tenth injection of AMPH. Comparison of the first and tenth AMPH injection also revealed clear evidence of sensitization to the stereotypy-inducing effects of AMPH that emerged 25 min post injection. The predominance of sensitization to the stereotypy-inducing effects of AMPH was also evident in the analysis of the sensitization index scores, which assessed the relative change in behavior on the last compared to the first injection of each animal. For ambulation, the scores for saline-treated rats (1.32 ± 0.17) were not significantly different from those for AMPH-treated rats (0.93 ± 0.14). For stereotypy, however, there were significant differences ($F_{1,10} = 5.94$, $p < 0.05$) between saline- and AMPH-treated rats (1.03 ±0.09 and 1.58 ± 0.15, respectively). Rats exhibiting behavioral sensitization were compared with normally behaving rats for the analysis of endogenous peptide levels in the dSTR, NA and mPFC, with tissue samples from these animals individually assayed for their peptide profiles.

Comparative analysis of the peptide compliment in different brain regions

To assess changes in the chemical state of the brain following AMPH-induced sensitization, we used MALDI-MS-based high-throughput exploratory analysis that did not focus on specific pathways nor require *a priori* information on the identity of the compound of interest. As postmortem degradation is inevitable in any experiment involving animal sacrifice (Fountoulakis *et al.* 2001), our larger goal was to ensure that sample quality was consistent across the entire sample set in order to allow comparisons of peptide profiles while minimizing sample to sample differences in postmortem proteolysis. We standardized the sampling approach to achieve as uniform a sample quality as possible when manually isolating tissues, and used a one-step DHB extraction method that extracts and preserves peptides, and minimizes loss due to sample handling (Romanova et al. 2008). With

optimized MS spectrum acquisition parameters, summation of technical duplicates, and normalization of signal intensity, we achieved reproducible measurements that led to insightful interrogation of biological samples. While 150–300 MS peaks were detected in the region-specific profiles, only a small subset of these putative peaks defined statistically significant differences between brain regions, and between saline- and AMPH-treated animals.

Our control set of samples when analyzed alone verified that the brain regions examined were reliably grouped by PCA, according to characteristic features found in the brain-region-specific mass spectral profiles. As shown on the PCA plot for the first three PCs in Fig. 3A, the dSTR, NA and mPFC samples were well segregated. In total, four PCs explained 98% of the variance among the control set of samples, PC1 ~81%, PC2 ~9%, PC3 ~5%, PC4 ~3%. The three-dimensional score plot for the first three PCs is shown in Fig. 3A, with PC1 indicating the most variability between morphologically different samples, and PC2 and PC3 accounting for variability between samples of the same kind. A follow-up ANOVA test revealed many known and putative peptides that were detected at statistically significant different levels, thus serving as features delineating the studied brain regions (Supporting Information, Table S1). Given the ability to classify region-specific peptide profiles in control samples, the AMPH-effected changes described next should represent true biological trends and not sampling artifacts.

When we compared the control (saline treated) and AMPH-treated samples, the entire data set (2 groups × 3 brain regions each) exhibited a degree of higher variability than the control group alone, which required six main PCs to describe the data (Fig. 3B). Distribution of the NAc and mPFC samples according to the treatment, saline or AMPH, is clear from the plot. Significant changes in the relative peak intensities that contributed to the observed segregation of peptide profiles between normally behaving and sensitized rats on the PCA plot are summarized in Fig. 4A–C. Statistical details on the specific peaks used in Fig. 4 for each brain region are included in the Supporting Information Tables S2–4. While not obvious from the PCA plot, a follow-up ANOVA test revealed several known truncated proteins detected at significantly higher intensities in the dSTR of AMPH-treated rats (Fig. 4A). Some of these marker peptides have been identified in the follow-up experiment described in the next section, and are listed in Table 1. As mPFC plays an important role in organizing behavior through functional regulation of numerous subcortical structures (Kolb 1984, Lindvall *et al.* 1978), it is not surprising that we find the largest number of peptide changes in the mPFC of sensitized rats (Fig. 4C). Among the observed peptides known to be modulated in the mPFC was an acetylated peptide from the PKC-interacting histidine triad nucleotide-binding protein 1 (Hint1) (Fig. 5), which increased nearly two-fold in signal intensity. In contrast, neuromodulin (P07936) peptide and a truncated form of synaptogyrin-1, a vesicle-associated membrane protein (Q62877), were found to decrease. We observed a 1.9–fold increase in the actin sequestering proteins thymosin beta-4 (P62329) and -10 (P63312) in both the NAc and mPFC following chronic AMPH exposure.

Multi-platform characterization of putative peptide markers

Using anatomically defined brain regions allowed us to lessen the anatomical complexity of the sample, improve the signal-to-noise ratio of MS measurements, and detect analytes unique to the brain region under investigation in the profiling experiments. We then pooled individual samples before their characterization so that greater effort could be directed to a larger combined sample, thereby facilitating our peptide identifications. Putative marker peptides were targeted for identification via multi-stage HPLC purification and MS/MS (Supporting Information, Tables S5 and S6). Implementing this tactic offered an advantage by allowing the multi-platform peptidome characterizations to be correlated with individual animal behavior. Not all of the peptides observed by MALDI-TOF MS profiling were

detected in the targeted sequencing experiments, and many of the sequenced peptides were not observed in the profiling experiments. We attribute this discrepancy to several reasons, including the documented 'complementary' nature of the ESI and MALDI platforms (Molle *et al.* 2009, Bodnar *et al.* 2003, Stapels & Barofsky 2004).

Likewise, pooling can present challenges due to the inherent cytological and chemical complexity of brain tissue, which complicates the chemical analyses of proteins and peptides at the tissue level. For example, if only a small population of cells in a tissue sample contain a compound of interest, then adding cells devoid of that compound makes its detection and identification difficult, in part, because the relative concentration of the particular analyte is reduced in a pooled sample. While our sequencing with LC-ESI-MS/MS used pooled samples in order to increase the amount of material available, the effects of dilution of low concentration, sparsely distributed peptides may have reduced those peptides below the instrumental detection limits, thus preventing their characterization. A number of distinct peptides were detected and characterized with each methodology using the pooled sample.

Individual variations in the behavioral response to chronic AMPH exposure have little effect on the classification of peptide profiles by PCA

Our individualized approach to the mass spectrometric analysis of tissue samples from the brain regions of individual animals allowed us to determine if there was a correlation between the variation in the behavioral responses to AMPH treatment and its effects on peptide levels in the studied brain regions. We used the mean ambulation and stereotypy values for the 60-min observation period post-injection, as well as the sensitization index, to identify each individual animal in order to enable tracking on the PCA plots of peptide profiles. When comparing the control and AMPH groups by brain region, we found that the PCA scores did not significantly correlate with either the behavioral scores or the sensitization index (data not shown). This finding suggests that, similar to the behavioral scores, the differences in peptide profiles are more profound between control and experimental groups than within the experimental group under the studied conditions. Alternatively, the relatively small size of our sample set (n = 4 for saline, n = 8 for AMPH), in combination with the broad range of behavioral responses (for the unsupervised PCA), may not be sufficient for finer classification within the AMPH group. There is a possibility that the effects we see are due to the final amphetamine injection, but these are more than likely influenced by the adaptations caused by repeated exposure to AMPH. Testing whether the differences in the PCA and sensitization scores may be due to the acute vs. chronic effects would require testing of additional groups; for example, one that received saline repeatedly and had a single challenge with AMPH, and one subjected to repeated AMPH exposures but receiving saline on the day of sacrifice. These experiments were not performed.

Discussion

As a substrate for transporters of biogenic amines, AMPH is known to produce long-lasting changes in neuronal structure and function in the PFC, NAc, and dSTR following repeated exposure (Kalivas *et al.* 2005, Kalivas & Volkow 2005). Enduring behavioral changes are widely reported as a response to chronic exposure to AMPH, and are considered to be mediated by drug-induced neuroadaptations within multiple brain regions that participate in the processing of reward (Chen *et al.* 2009). In this work, we probed the neurochemical changes in three of these regions—the dSTR, NA, and PFC—using a rodent model of AMPH-induced sensitization. Our data indicate that despite the overlapping peaks detected via MALDI-TOF MS, the dSTR, NAc and mPFC have differences in the composition and/or abundance of the detectable peptides, and these distinctions are sufficient for categorizing each brain region.

The majority of peptides detected in this study represent truncated forms of previously characterized proteins, some of which we earlier reported in isolated rat brain regions (Romanova et al. 2010). Because peptides with altered levels in the AMPH-sensitized rats originate from functionally characterized proteins, one can speculate on the neural pathways perturbed by repeated AMPH exposure. The results of this MS-based, non-candidate and label-free screening of AMPH-induced alterations in peptide levels in specific brain regions point to changes in pathways that regulate energy/metabolism, neurotransmission, apoptosis, neuroprotection, neuritogenesis, and cytoskeleton integrity. In what follows, the protein connections to drug-induced neuroadaptation are discussed.

It is well known that robust sensitization to psychomotor activation following chronic exposure to AMPH is associated with structural changes in the brain, such as alterations in synaptic connectivity and neuronal morphology in regions that mediate the drug's psychomotor activating and rewarding effects (Robinson & Kolb 1997, Singer *et al.* 2009). The dynamic architecture of actin, maintained by the polymerization and depolymerization of actin filaments by severing proteins, plays a significant role in these drug-induced structural changes via alterations in the morphology of dendritic spines (Toda *et al.* 2006). Thymosin beta-4 is widely distributed in the nervous system and has multiple biological activities that collectively contribute to wound healing in numerous tissues, as observed in various animal models (Huff *et al.* 2001, Philp & Kleinman 2010). This intriguing, small protein plays a role in synaptogenesis, axon growth, cell migration and plastic changes in the CNS. It also appears to promote the survival and neurite outgrowth of cultured neurons (Philp & Kleinman 2010, Yang *et al.* 2010, Romanova *et al.* 2006, Yang *et al.* 2008a) and is considered a candidate neurorestorative agent (Morris *et al.* 2010). Thymosin beta-4 has also been shown to offset ethanol-induced neurotoxicity in cultured cortical astrocytes through inhibition of apoptosis signaling (Yang et al. 2010). One of the mechanisms underlying the capacity of thymosin beta-4 to suppress apoptosis may in part be due to its anti-peroxidation effect. In contrast to thymosin beta-4, thymosin beta-10 is known as an actin-mediated tumor suppressor and acts as potent inhibitor of angiogenesis (Lee *et al.* 2005). Collectively, thymosin beta-4 and -10 may prevent apoptosis of neurons via blockade of early apoptogenic signals that are independent of actin remodeling actions (Choi *et al.* 2006) The two-fold increase in signal intensity observed from thymosin beta-4 and -10 in the AMPH-treated rats in our study provides further evidence for the role of cytoskeleton integrity in the AMPH-induced neuroadaptations.

Relevant to the structural integrity of the CNS under AMPH exposure are the changes in stathmin levels. A cytoplasmic phosphoprotein involved in plastic adaptation that is also known as a marker for neuritic sprouting (Himi *et al.* 1994, Sobel 1991), stathmin binds to microtubules and inhibits their assembly, resulting in neuritogenesis through the regulation of dynamic microtubule instability (Belmont & Mitchison 1996). Stathmin mRNA levels have previously been reported to increase after acute exposure to AMPH (Hiroshi *et al.* 2002). We recently showed that increased levels of acetylated stathmin peptide (ac)ASSDIQVKELEKRASGQAFEL are associated with reduced sensitivity to the behavioral effects of cocaine in rats (Romanova et al. 2010). Collectively, these previously reported observations and our finding here of increased stathmin-derived peptide levels in the NAc after AMPH treatment, support the hypothesis that rearrangement and structural modification of neural networks in the brain are likely involved in behavioral sensitization.

A growing dataset provides extensive evidence of a connection between psychostimulant exposure and myelin integrity in the nervous system (Melo *et al.* 2006, Chang *et al.* 2007, Romanova et al. 2010, Albertson *et al.* 2006, Marshall *et al.* 2007). Our finding of a decreased level of myelin basic protein-related peptide may reflect compromised myelination of striatal neurons that could have developed with chronic exposure to lower

doses of AMPH over time. Levels of a truncated form of a neuron-specific polypeptide, PEP-19 (Slemmon *et al.* 1996), were also altered. One plausible explanation supporting this observation is that PEP-19 binds to calmodulin through the IQ motif in a Ca^{2+}-independent manner (Slemmon et al. 1996, Putkey *et al.* 2003) and is thought to exert neuroprotective effects in apoptosis by blocking several calmodulin-dependent pathways (Erhardt *et al.* 2000).

A group of peptides detected at altered levels in the AMPH-treated rats originates from proteins known to be involved in neurogenesis; e.g., decreased neuromodulin in the mPFC, thought to be involved in neurite plasticity in the late phase of stimulant-induced sensitization (Gnegy *et al.* 1993), and synaptogyrin-1, a vesicle-associated membrane protein. Reduced expression of synaptogyrin-1 has been reported in postmortem brains of schizophrenia patients (Cheng & Chen 2007). Similar to AMPH-induced behavioral sensitization, the etiology of schizophrenia involves alterations in neuronal functions associated with dopaminergic signaling (Heinz & Schlagenhauf 2010).

Interestingly, the most dramatic differences between the control and AMPH-treated rats were changes in the levels of the Hint1 peptide. An increased level of Hint1 peptide was recently reported by us in mPFC extracts from rats given a single injection of cocaine and was linked to the “low cocaine responder” behavioral phenotype (Romanova et al. 2010). Additional evidence points to the role of Hint1 in modulating the effects of a number of drugs of abuse. For example, Hint1 specifically interacts with the C-terminus of the μ-opioid receptor, modulates receptor desensitization, and inhibits PKC-mediated μ-opioid receptor phosphorylation (Guang *et al.* 2004). Hint1 knockout mice have an altered postsynaptic dopamine function that modulates the behavioral response to AMPH (Barbier *et al.* 2007). Further, with association, expression, and molecular studies, Jackson and colleagues (Jackson *et al.* 2010) demonstrated that nicotine-induced modulation of Hint1 levels may be involved in the mechanisms of excess smoking in humans.

A few studies link alterations in energy metabolism to neuronal death, neurodegeneration, and psychiatric disorders, including schizophrenia and drug abuse (Cunha-Oliveira *et al.* 2006, Lehrmann & Freed 2008, Lehrmann *et al.* 2003, Burrows *et al.* 2000) through a possible malfunction in the biochemical cascade (for review, see (Rezin *et al.* 2009)). In agreement with this hypothesis, we detected reduced levels of the ubiquitous subunit of cytochrom C oxidase, Cox7c, which is expressed in all tissues and is related to mitochondrial metabolic function (Lenka *et al.* 1998).

Conclusions

Using modification of the behavioral response to AMPH as a model selection criterion, we found dynamic subsets of peptides in three regions of the brain’s reward circuitry that were altered under chronic AMPH treatment. Our results demonstrate that behavioral sensitization to AMPH is associated with complex chemical adaptations in the brain reward circuit in pathways that regulate energy/metabolism, neurotransmission, apoptosis, neuroprotection, and neuritogenesis, as well as cytoskeleton integrity and neuronal morphology. The marker peptides identified here originated from proteins that have been recognized for their roles in neuroadaptation and drug-induced behavioral sensitization in humans and rodents, as well as several intriguing peptides and proteins not previously associated with the effects of repeated exposure to illicit drugs. These unexpected peptides may become potential new pharmacological targets for treatment of AMPH dependence and toxicity. Overall, the data imply that chemical changes in neuronal organization and pathways other than the mesolimbic dopamine system contribute to the effect of chronic AMPH exposure on behavior.

Supplementary Material

Refer to Web version on PubMed Central for supplementary material.

Acknowledgments

We thank Dr. Leonid Zamdborg for helpful discussions on the FTMS data analysis, Jessica Stanis for help with behavioral testing and brain tissue sampling, and Dr. Sandra Rodriguez-Zas for a critical review of the PCA results. The project was supported by a gift from the Roy J. Carver Charitable Trust and Award Numbers Award Numbers DA018310, DA017940, and DA029815 from the National Institute on Drug Abuse (NIDA). The content is solely the responsibility of the authors and does not necessarily represent the official views of NIDA or the National Institutes of Health.

Abbreviations used

AMPH	amphetamine
CapLC	capillary liquid chromatography
DHB	2,5-dihydroxybenzoic acid
dSTR	dorsal striatum
ESI	electrospray ionization
FA	formic acid
FTMS	Fourier transform mass spectrometry
HFBA	heptafluorobutyric acid
LC	liquid chromatography
MALDI	matrix-assisted laser desorption/ionization
MS	mass spectrometry
MS/MS	tandem mass spectrometry
NAc	nucleus accumbens
PCA	principal component analysis
mPFC	medial prefrontal cortex
SPE	solid phase extraction
TOF	time-of-flight
VTA	ventral tegmental area

References

Abul-Husn NS, Devi LA. Neuroproteomics of the synapse and drug addiction. J Pharmacol Exp Ther. 2006; 318:461–468. [PubMed: 16644901]

Albertson DN, Schmidt CJ, Kapatos G, Bannon MJ. Distinctive profiles of gene expression in the human nucleus accumbens associated with cocaine and heroin abuse. Neuropsychopharmacology. 2006; 31:2304–2312. [PubMed: 16710320]

Barbier E, Zapata A, Oh E, Liu Q, Zhu F, Undie A, Shippenberg T, Wang JB. Supersensitivity to amphetamine in protein kinase-C interacting protein/HINT1 knockout mice. Neuropsychopharmacology. 2007; 32:1774–1782. [PubMed: 17203012]

Bartlett E, Hallin A, Chapman B, Angrist B. Selective sensitization to the psychosis-inducing effects of cocaine: a possible marker for addiction relapse vulnerability? Neuropsychopharmacology. 1997; 16:77–82. [PubMed: 8981391]

Belmont LD, Mitchison TJ. Identification of a protein that interacts with tubulin dimers and increases the catastrophe rate of microtubules. Cell. 1996; 84:623–631. [PubMed: 8598048]

Bodnar WM, Blackburn RK, Krise JM, Moseley MA. Exploiting the complementary nature of LC/MALDI/MS/MS and LC/ESI/MS/MS for increased proteome coverage. J Am Soc Mass Spectrom. 2003; 14:971–979. [PubMed: 12954165]

Boileau I, Dagher A, Leyton M, Gunn RN, Baker GB, Diksic M, Benkelfat C. Modeling sensitization to stimulants in humans: an [11C]raclopride/positron emission tomography study in healthy men. Arch Gen Psychiatry. 2006; 63:1386–1395. [PubMed: 17146013]

Boyne MT, Garcia BA, Li M, Zamdborg L, Wenger CD, Babai S, Kelleher NL. Tandem mass spectrometry with ultrahigh mass accuracy clarifies peptide identification by database retrieval. J Proteome Res. 2009; 8:374–379. [PubMed: 19053528]

Brereton, R. Chemometrics for Pattern Recognition. John Wiley & Sons, Ltd; 2009.

Burrows KB, Gudelsky G, Yamamoto BK. Rapid and transient inhibition of mitochondrial function following methamphetamine or 3,4-methylenedioxymethamphetamine administration. Eur J Pharmacol. 2000; 398:11–18. [PubMed: 10856443]

Chang L, Alicata D, Ernst T, Volkow N. Structural and metabolic brain changes in the striatum associated with methamphetamine abuse. Addiction. 2007; 102(Suppl 1):16–32. [PubMed: 17493050]

Chen BT, Hopf FW, Bonci A. Synaptic plasticity in the mesolimbic system. Ann N Y Acad Sci. 2009; 1187:129–139. [PubMed: 20201850]

Cheng MC, Chen CH. Identification of rare mutations of synaptogyrin 1 gene in patients with schizophrenia. J Psychiatric Res. 2007; 41:1027–1031.

Choi SY, Kim DK, Eun B, Kim K, Sun W, Kim H. Anti-apoptotic function of thymosin-beta in developing chick spinal motoneurons. Biochem Biophys Res Commun. 2006; 346:872–878. [PubMed: 16782066]

Cunha-Oliveira T, Rego AC, Cardoso SM, Borges F, Swerdlow RH, Macedo T, de Oliveira CR. Mitochondrial dysfunction and caspase activation in rat cortical neurons treated with cocaine or amphetamine. Brain Res. 2006; 1089:44–54. [PubMed: 16638611]

Darde VM, de la Cuesta F, Dones FG, Alvarez-Llamas G, Barderas MG, Vivanco F. Analysis of the plasma proteome associated with acute coronary syndrome: does a permanent protein signature exist in the plasma of ACS patients? J Proteome Res. 2010; 9:4420–4432. [PubMed: 20597552]

Dudoit S, Shaffer JP. Multiple hypothesis testing in microarray experiments. Stat Sci. 2003; 18:71–103.

Erhardt JA, Legos JJ, Johanson RA, Slemmon JR, Wang X. Expression of PEP-19 inhibits apoptosis in PC12 cells. Neuroreport. 2000; 11:3719–3723. [PubMed: 11117479]

Faure JJ, Hattingh SM, Stein DJ, Daniels WM. Proteomic analysis reveals differentially expressed proteins in the rat frontal cortex after methamphetamine treatment. Metab Brain Dis. 2009; 24:685–700. [PubMed: 19826936]

Fenn JB, Mann M, Meng CK, Wong SF, Whitehouse CM. Electrospray ionization for mass spectrometry of large biomolecules. Science. 1989; 246:64–71. [PubMed: 2675315]

Fountoulakis M, Hardmeier R, Hoger H, Lubec G. Postmortem changes in the level of brain proteins. Exp Neurol. 2001; 167:86–94. [PubMed: 11161596]

Fricker LD, Lim J, Pan H, Che FY. Peptidomics: identification and quantification of endogenous peptides in neuroendocrine tissues. Mass Spectrom Rev. 2006; 25:327–344. [PubMed: 16404746]

Gnegy ME, Hong P, Ferrell ST. Phosphorylation of neuromodulin in rat striatum after acute and repeated, intermittent amphetamine. Mol Brain Res. 1993; 20:289–298. [PubMed: 8114616]

Guang W, Wang H, Su T, Weinstein IB, Wang JB. Role of mPKCI, a novel mu-opioid receptor interactive protein, in receptor desensitization, phosphorylation, and morphine-induced analgesia. Mol Pharmacol. 2004; 66:1285–1292. [PubMed: 15496510]

Hanrieder J, Wicher G, Bergquist J, Andersson M, Fex-Svenningsen A. MALDI mass spectrometry based molecular phenotyping of CNS glial cells for prediction in mammalian brain tissue. Anal Bioanal Chem. 2011; 401:135–147. [PubMed: 21553124]

Heinz A, Schlagenhauf F. Dopaminergic dysfunction in schizophrenia: salience attribution revisited. Schizophr Bull. 2010; 36:472–485. [PubMed: 20453041]

Hillenkamp, F.; Karas, M. The MALDI process and method. In: Hillenkamp, F.; Peter-Katalini, J., editors. A Practical Guide to Instrumentation, Methods and Applications. Wiley-VCH Verlag GmbH & Co. KGaA; Weinheim, Germany: 2007.

Himi T, Okazaki T, Wang H, McNeill TH, Mori N. Differential localization of SCG10 and p19/stathmin messenger RNAs in adult rat brain indicates distinct roles for these growth-associated proteins. Neuroscience. 1994; 60:907–926. [PubMed: 7936211]

Hiroshi U, Manabu T, Masafumi K, Shigetoshi K. Gene expression related to synaptogenesis, neuritogenesis, and MAP kinase in behavioral sensitization to psychostimulants. Ann N Y Acad Sci. 2002; 965:55–67. [PubMed: 12105085]

Huff T, Muller CSG, Otto AM, Netzker R, Hannappel E. [beta]-Thymosins, small acidic peptides with multiple functions. Int J Biochem Cell Biol. 2001; 33:205–220. [PubMed: 11311852]

Jackson KJ, Chen Q, Chen J, Aggen SH, Kendler KS, Chen X. Association of the histidine-triad nucleotide-binding protein-1 (HINT1) gene variants with nicotine dependence. Pharmacogenomics J. 2010; 11:251–257. [PubMed: 20514075]

Kalivas PW, Pierce RC, Cornish J, Sorg BA. A role for sensitization in craving and relapse in cocaine addiction. J Psychopharmacol. 1998; 12:49–53. [PubMed: 9584968]

Kalivas PW, Volkow N, Seamans J. Unmanageable motivation in addiction: a pathology in prefrontal-accumbens glutamate transmission. Neuron. 2005; 45:647–650. [PubMed: 15748840]

Kalivas PW, Volkow ND. The neural basis of addiction: a pathology of motivation and choice. Am J Psychiatry. 2005; 162:1403–1413. [PubMed: 16055761]

Kolb B. Functions of the frontal cortex of the rat: a comparative review. Brain Res Rev. 1984; 8:65–98.

Kruskal WH, Wallis WA. Use of ranks in one-criterion variance analysis. J Amer Stat Assoc. 1952; 47:588–621.

Lee JE, Atkins N Jr, Hatcher NG, Zamdborg L, Gillette MU, Sweedler JV, Kelleher NL. Endogenous peptide discovery of the rat circadian clock: a focused study of the suprachiasmatic nucleus by ultrahigh performance tandem mass spectrometry. Mol Cell Proteomics. 2010; 9:285–297. [PubMed: 19955084]

Lee SH, Son MJ, Oh SH, Rho SB, Park K, Kim YJ, Park MS, Lee JH. Thymosin {beta}(10) inhibits angiogenesis and tumor growth by interfering with Ras function. Cancer Res. 2005; 65:137–148. [PubMed: 15665289]

Lehrmann E, Freed WJ. Transcriptional correlates of human substance use. Ann N Y Acad Sci. 2008; 1139:34–42. [PubMed: 18991846]

Lehrmann E, Oyler J, Vawter MP, Hyde TM, Kolachana B, Kleinman JE, Huestis MA, Becker KG, Freed WJ. Transcriptional profiling in the human prefrontal cortex: evidence for two activational states associated with cocaine abuse. Pharmacogenomics J. 2003; 3:27–40. [PubMed: 12629581]

Lenka, N.; Vijayasarathy, C.; Mullick, J.; Avadhani, NG.; Kivie, M. Prog Nucleic Acid Res Mol Biol. Vol. 61. Academic Press; 1998. Structural organization and transcription regulation of nuclear genes encoding the mammalian cytochrome c oxidase complex; p. 309-344.

Li L, Sweedler JV. Peptides in the brain: mass spectrometry-based measurement approaches and challenges. Annu Rev Anal Chem (Palo Alto, Calif). 2008; 1:451–483. [PubMed: 20636086]

Lindvall O, Bjorklund A, Divac I. Organization of catecholamine neurons projecting to the frontal cortex in the rat. Brain Res. 1978; 142:1–24. [PubMed: 626911]

Marshall JF, Belcher AM, Feinstein EM, O'Dell SJ. Methamphetamine-induced neural and cognitive changes in rodents. Addiction. 2007; 102(Suppl 1):61–69. [PubMed: 17493054]

Melo P, Moreno VZ, Vazquez SP, Pinazo-Duran MD, Tavares MA. Myelination changes in the rat optic nerve after prenatal exposure to methamphetamine. Brain Res. 2006; 1106:21–29. [PubMed: 16842764]

Molle D, Jardin J, Piot M, Pasco M, Leonil J, Gagnaire V. Comparison of electrospray and matrix-assisted laser desorption ionization on the same hybrid quadrupole time-of-flight tandem mass spectrometer: application to bidimensional liquid chromatography of proteins from bovine milk fraction. J Chromatogr. 2009; 1216:2424–2432.

Morris DC, Chopp M, Zhang L, Zhang ZG. Thymosin beta4: a candidate for treatment of stroke? Ann N Y Acad Sci. 2010; 1194:112–117. [PubMed: 20536457]

Paxinos, G.; Watson, C. The Rat Brain in Stereotaxic Coordinates. Academic Press; 2007.

Philp D, Kleinman HK. Animal studies with thymosin beta, a multifunctional tissue repair and regeneration peptide. Ann N Y Acad Sci. 2010; 1194:81–86. [PubMed: 20536453]

Putkey JA, Kleerekoper Q, Gaertner TR, Waxham MN. A new role for IQ motif proteins in regulating calmodulin function. J Biol Chem. 2003; 278:49667–49670. [PubMed: 14551202]

Rajalahti T, Kroksveen AC, Arneberg R, Berven FS, Vedeler CA, Myhr KM, Kvalheim OM. A multivariate approach to reveal biomarker signatures for disease classification: application to mass spectral profiles of cerebrospinal fluid from patients with multiple sclerosis. J Proteome Res. 2010; 9:3608–3620. [PubMed: 20499859]

Rezin G, Amboni G, Zugno A, Quevedo J, Streck E. Mitochondrial dysfunction and psychiatric disorders. Neurochem Res. 2009; 34:1021–1029. [PubMed: 18979198]

Robinson TE, Becker JB, Moore CJ, Castaneda E, Mittleman G. Enduring enhancement in frontal cortex dopamine utilization in an animal model of amphetamine psychosis. Brain Res. 1985; 343:374–377. [PubMed: 4052758]

Robinson TE, Berridge KC. The neural basis of drug craving: an incentive-sensitization theory of addiction. Brain Res Brain Res Rev. 1993; 18:247–291. [PubMed: 8401595]

Robinson TE, Berridge KC. The psychology and neurobiology of addiction: an incentive-sensitization view. Addiction. 2000; 95(Suppl 2):S91–117. [PubMed: 11002906]

Robinson TE, Kolb B. Persistent structural modifications in nucleus accumbens and prefrontal cortex neurons produced by previous experience with amphetamine. J Neurosci. 1997; 17:8491–8497. [PubMed: 9334421]

Romanova EV, Hatcher NG, Rubakhin SS, Sweedler JV. Characterizing intercellular signaling peptides in drug addiction. Neuropharmacology. 2009; 56(Suppl 1):196–204. [PubMed: 18722391]

Romanova EV, Lee JE, Kelleher NL, Sweedler JV, Gulley JM. Mass spectrometry screening reveals peptides modulated differentially in the medial prefrontal cortex of rats with disparate initial sensitivity to cocaine. AAPS J. 2010; 12:443–454. [PubMed: 20490734]

Romanova EV, Roth MJ, Rubakhin SS, Jakubowski JA, Kelley WP, Kirk MD, Kelleher NL, Sweedler JV. Identification and characterization of homologues of vertebrate beta-thymosin in the marine mollusk *Aplysia californica*. J Mass Spectrom. 2006; 41:1030–1040. [PubMed: 16924592]

Romanova EV, Rubakhin SS, Sweedler JV. One-step sampling, extraction, and storage protocol for peptidomics using dihydroxybenzoic acid. Anal Chem. 2008; 80:3379–3386. [PubMed: 18321135]

Rossbach U, Nilsson A, Falth M, Kultima K, Zhou Q, Hallberg M, Gordh T, Andren PE, Nyberg F. A quantitative peptidomic analysis of peptides related to the endogenous opioid and tachykinin systems in nucleus accumbens of rats following naloxone-precipitated morphine withdrawal. J Proteome Res. 2009; 8:1091–1098. [PubMed: 19159213]

Segal, DS.; Schuckit, MA. Animal models of stimulant-induced psychosis. In: Creese, I., editor. Stimulants: Neurochemical, Behavioral, and Clinical Perspectives. Raven Press; New York: 1983. p. 131-167.

Singer BF, Tanabe LM, Gorny G, Jake-Matthews C, Li Y, Kolb B, Vezina P. Amphetamine-induced changes in dendritic morphology in rat forebrain correspond to associative drug conditioning rather than nonassociative drug sensitization. Biol Psychiatry. 2009; 65:835–840. [PubMed: 19200535]

Slemmon JR, Morgan JI, Fullerton SM, Danho W, Hilbush BS, Wengenack TM. Camstatins are peptide antagonists of calmodulin based upon a conserved structural motif in PEP-19, neurogranin, and neuromodulin. J Biol Chem. 1996; 271:15911–15917. [PubMed: 8663125]

Sobel A. Stathmin: a relay phosphoprotein for multiple signal transduction? Trends Biochem Sci. 1991; 16:301–305. [PubMed: 1957351]

Stanis JJ, Marquez Avila H, White MD, Gulley JM. Dissociation between long-lasting behavioral sensitization to amphetamine and impulsive choice in rats performing a delay-discounting task. Psychopharmacology. 2008; 199:539–548. [PubMed: 18473112]

Stapels M, Barofsky D. Complementary use of MALDI and ESI for the HPLC-MS/MS analysis of DNA-binding proteins. Anal Chem. 2004; 76:5423–5430. [PubMed: 15362902]

Stephens MA. EDF for goodness of fit and some comparisons. J Amer Stat Assoc. 1974; 69:730–737.

Strakowski SM, DelBello MP, Adler CM. Comparative efficacy and tolerability of drug treatments for bipolar disorder. CNS Drugs. 2001; 15:701–718. [PubMed: 11580309]

Svensson M, Skold K, Nilsson A, Falth M, Svenningsson P, Andren PE. Neuropeptidomics: expanding proteomics downwards. Biochem Soc Trans. 2007; 35:588–593. [PubMed: 17511658]

Toda S, Shen HW, Peters J, Cagle S, Kalivas PW. Cocaine increases actin cycling: effects in the reinstatement model of drug seeking. J Neurosci. 2006; 26:1579–1587. [PubMed: 16452681]

Ujike H, Sato M. Clinical features of sensitization to methamphetamine observed in patients with methamphetamine dependence and psychosis. Ann N Y Acad Sci. 2004; 1025:279–287. [PubMed: 15542728]

Uys JD, Grey AC, Wiggins A, Schwacke JH, Schey KL, Kalivas PW. Matrix-assisted laser desorption/ionization tissue profiling of secretoneurin in the nucleus accumbens shell from cocaine-sensitized rats. J Mass Spectrom. 2010; 45:97–103. [PubMed: 19918966]

Wei H, Nolkrantz K, Parkin MC, Chisolm CN, O'Callaghan JP, Kennedy RT. Identification and quantification of neuropeptides in brain tissue by capillary liquid chromatography coupled off-line to MALDI-TOF and MALDI-TOF/TOF-MS. Anal Chem. 2006; 78:4342–4351. [PubMed: 16808441]

Wilcoxon F. Individual comparisons by ranking methods. Biometrics. 1945; 1:80–83.

Yang H, Cheng X, Yao Q, Li J, Ju G. The promotive effects of thymosin β4 on neuronal survival and neurite outgrowth by upregulating L1 expression. Neurochem Res. 2008a; 33:2269–2280. [PubMed: 18461449]

Yang H, Cui GB, Jiao XY, Wang J, Ju G, You SW. Thymosin-beta4 attenuates ethanol-induced neurotoxicity in cultured cerebral cortical astrocytes by inhibiting apoptosis. Cell Mol Neurobiol. 2010; 30:149–160. [PubMed: 19688260]

Yang MH, Kim S, Jung MS, et al. Proteomic analysis of methamphetamine-induced reinforcement processes within the mesolimbic dopamine system. Addict Biol. 2008b; 13:287–294. [PubMed: 18279499]

Zvonok N, Xu W, Williams J, Janero DR, Krishnan SC, Makriyannis A. Mass spectrometry-based GPCR proteomics: comprehensive characterization of the human cannabinoid 1 receptor. J Proteome Res. 2010; 9:1746–1753. [PubMed: 20131867]

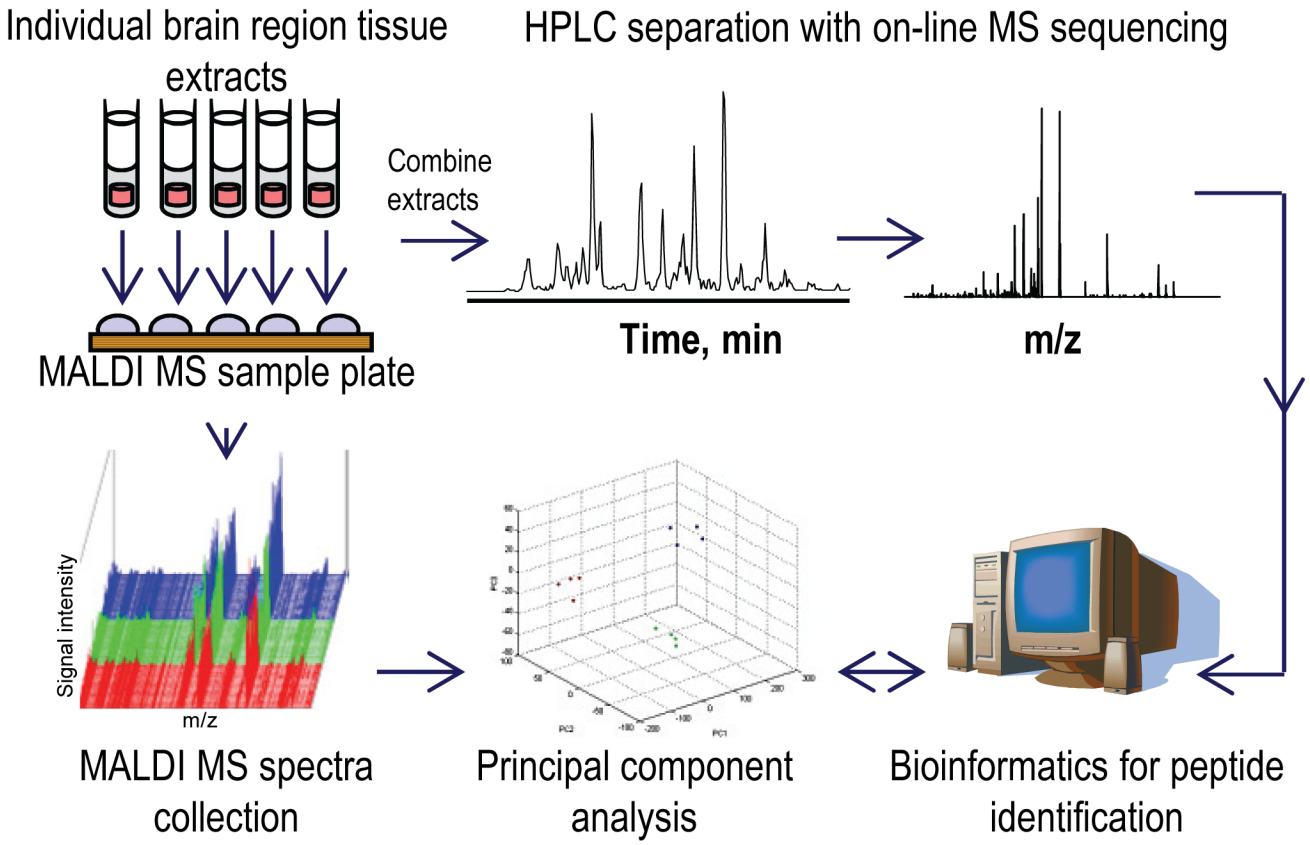

Fig. 1.

Experimental workflow for comparative peptidomics of individual brain region samples. Individual tissue samples were processed via a one-step peptide extraction method. Peptide profiles of individual peptide extracts were obtained by high throughput MALDI-TOF MS measurements. Mass spectral profiles of different brain regions and experimental groups were compared statistically using principal component analysis followed by either ANOVA or t-test to reveal potential biomarker peptides. Biomarker peptides were then identified via mass spectrometric sequencing using LC-MS/MS and database searches.

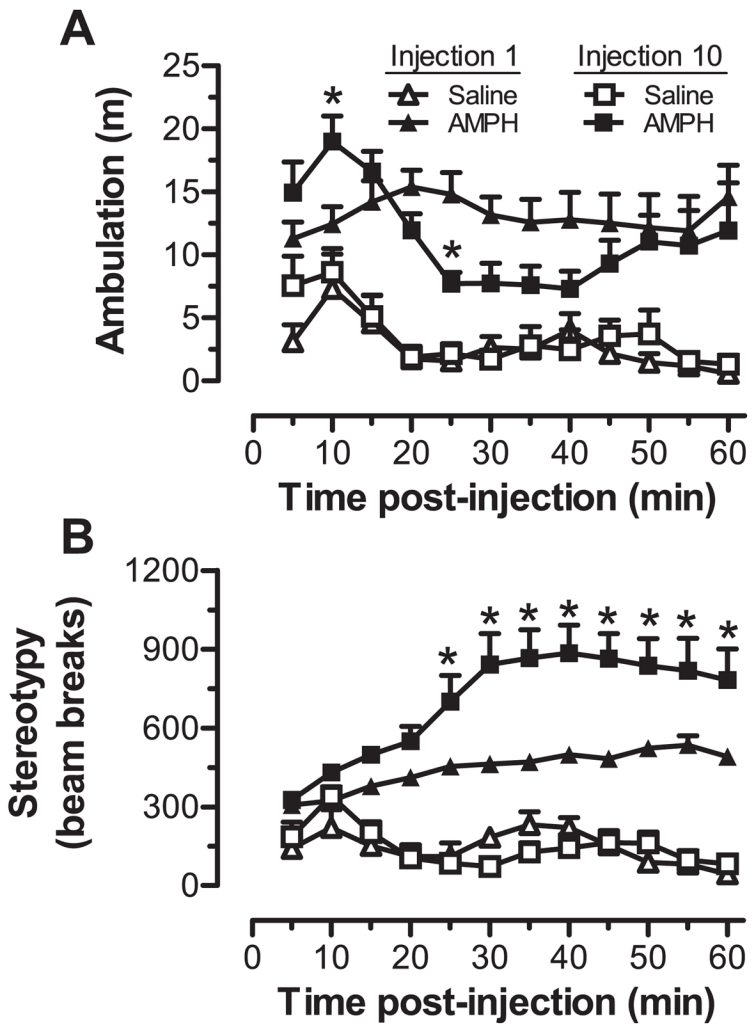

Fig. 2.

Individual animal behavioral tests included both **(A)** ambulatory distance and **(B)** stereotypy, here shown after the first and tenth injection of saline (n = 4) or 3.0 mg/kg *d*-amphetamine (n = 8; AMPH). Ambulation was quantified by photobeam breaks that resulted in a coordinate change within the open-field arena but were not repetitive in nature. Stereotypy movements were quantified by photobeam breaks that were repetitive and did not result in large location changes that were progressively further from the starting point of movement. *$p < 0.05$, compared to injection 1 at the indicated time point.

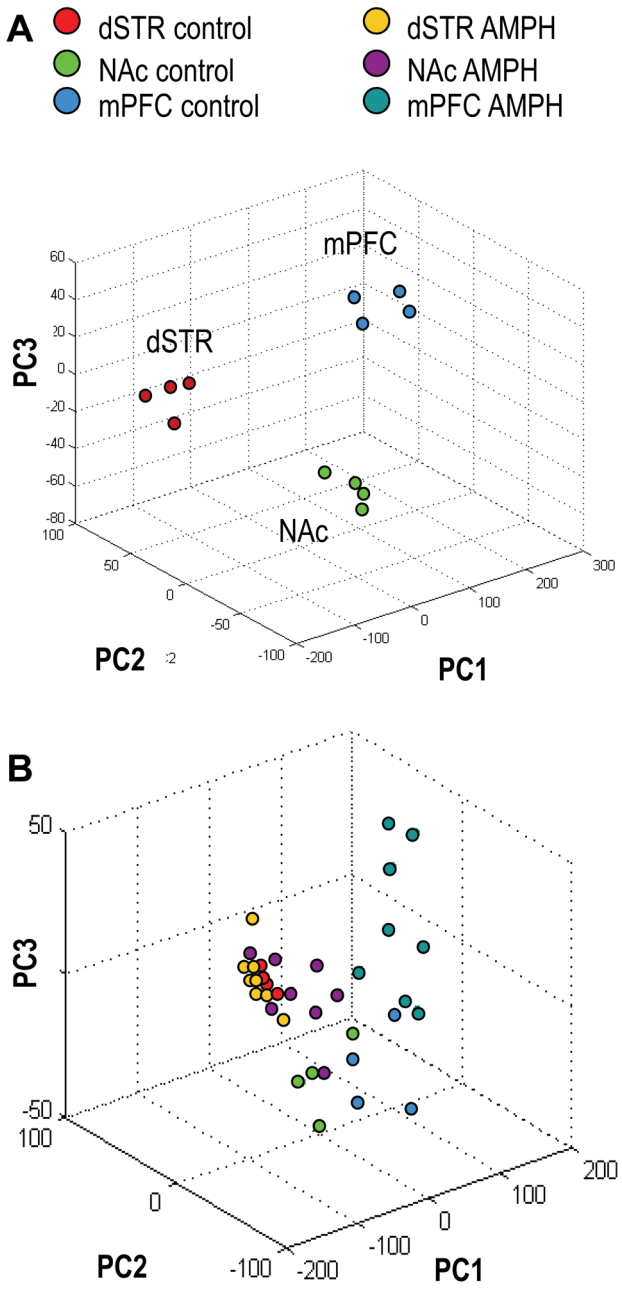

Fig. 3.

Classification of brain regions from the control group and AMPH group of animals by peptide profiles using principal component analysis (PCA). **(A)** PCA score plot for the control group of animals. Four principal components (PCs) explain 98% of variance, PC1 ~81%, PC2 ~9%, PC3 ~5%, PC4 ~3%, but only 3 PCs are shown. **(B)** PCA score plot for the AMPH-treated and control groups of rats. Six PCs explain >95% of variance: PC1 ~70%, PC2 ~12%, residual variance is accounted for by PC3–PC6. Only the first 3 PCs are plotted. dSTR – dorsal striatum, NAc – nucleus accumbens, mPFC – medial prefrontal cortex. Each data point represents an individual animal.

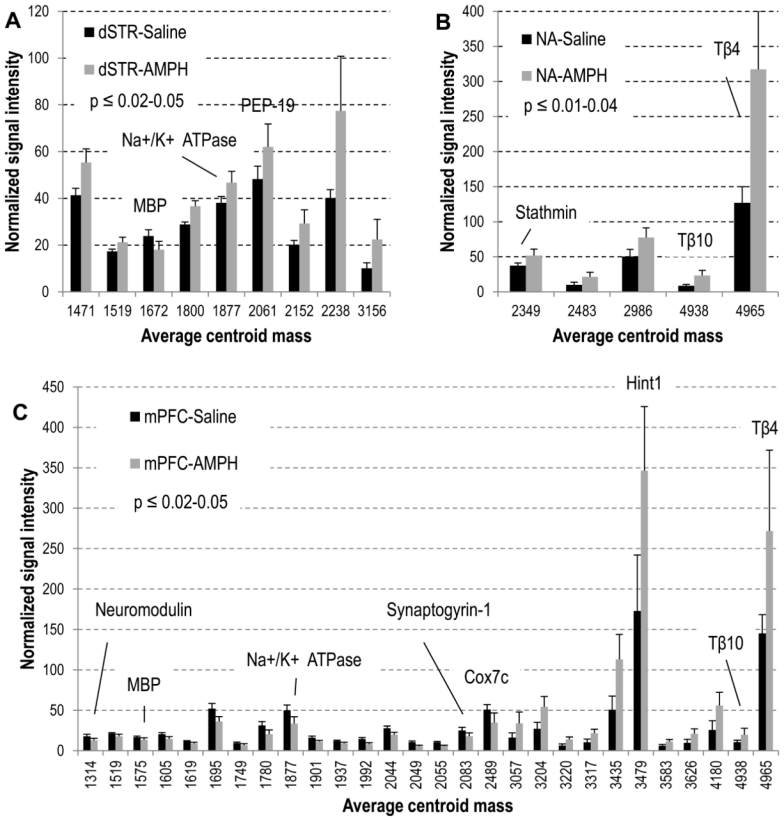

Fig. 4.

Relative peak intensities of putative peptides detected at statistically significant different levels in rats treated chronically with 3.0 mg/kg AMPH: **(A)** dorsal striatum, **(B)** nucleus accumbens, **(C)** medial prefrontal cortex. Peaks are listed as an average centroid mass at the half width/maximum height of the integration region for peak picking on the cumulative processed group spectrum; the p-value is calculated for normally distributed data; error bars represent standard deviation; p = 0.06 for peptides *m/z* 1672 and 2061 on **(A).** Peptides identified in the follow-up peptidomics experiments are labeled.

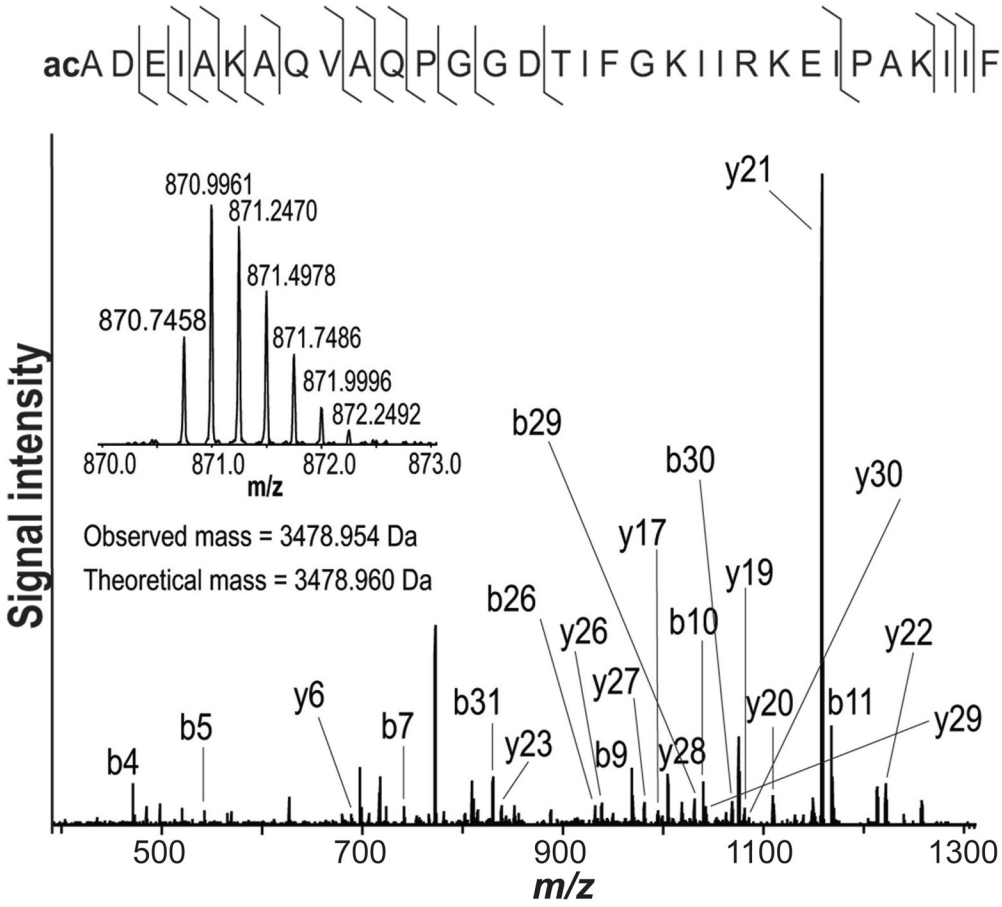

Fig. 5.

Identification of histidine triad nucleotide-binding protein 1 (Hint1) via its acetylated peptide (2–33). The fragmentation spectrum shows the unambiguous identification of the complementary ion series; the insert shows the isolation of the quadruple-charged ion of Hint1 peptide.

Table 1

List of identified marker peptides correlated with chronic AMPH treatment.

Accession	Protein name	Detected peptide	Mass	Brain region
P62329	Thymosin beta-4	**ac**SDKPDMAEIEKFDKSKLKKTETQEKNPLP SKETIEQEKQAGES	4965.16	NA, mPFC
P63312	Thymosin beta-10	**ac**ADKPDMGEIASFDKAKLKKTETQEKNTLP TKETIEQEKRSEIS	4938.08	NA, mPFC
P13668	Stathmin	**ac**ASSDIQVKELEKRASGQFEL	2349.47	NA
P02688	Myelin basic protein S	KLGGRDSRGSPMAR	1575.24	mPFC
Q8CHN7	PEP-19	DIDMDAPETERAAVAIQSQ	2061.25	dSTR
B2RYT3	Cox7c protein	SHYEEGPGKNLPFSVENKWRL	2488.72	mPFC
P02688	Myelin basic protein S	**ac**ASQKRPSQRHGSKY	1672.44	dSTR
P07936	Neuromodulin	APVADGVEKKEGD	1314.23	mPFC
P13638	Na+/K+ ATPase subunit beta-2	RVAPPGLTQIPQIQKTE	1877.05	dSTR, mPFC
P62959	Histidine triad nucleotide-binding protein 1	**ac**ADEIAKAQVAQPGGDTIFGKIIRKEIPAKIIF	3478.95	mPFC
Q62877	Synaptogyrin-1	PSQDSSMPYAPYVEPSAGSD	2083.33	mPFC

Mass is the centroid of the average protonated molecular ion peak found on the cumulative processed group spectrum used for comparative statistical analysis.

ac = acetylation.